Imaging the electro-kinetic response of biological tissues with optical coherence tomography

K. Wawrzyn,[1,†] V. Demidov,[1,†] B. Vuong,[2] M. K. Harduar,[2] C. Sun,[2,3] V. X. D. Yang,[2,4] O. Doganay,[1] V. Toronov,[1] and Y. Xu[1,*]

[1]Department of Physics, Ryerson University, Toronto, Canada

[2]Department of Electrical and Computer Engineering Ryerson University, Toronto, Canada

[3]Department of Medicine, University of Toronto, Toronto, Canada

[4]Division of Neurosurgery, University of Toronto, Toronto, Canada

*Corresponding author: yxu@ryerson.ca

Received April 22, 2013; revised June 6, 2013; accepted June 10, 2013; posted June 14, 2013 (Doc. ID 189149); published July 12, 2013

We demonstrate the feasibility of using optical coherence tomography (OCT) to detect and image an electro-kinetic response: electric-field induced optical changes (EIOC) in soft biological tissues. A low-frequency electric field was applied to *ex vivo* samples of porcine heart tissues, while OCT signals were acquired continuously. Experimental results show that the amplitude of the OCT signal change is proportional to the amplitude and inversely proportional to the frequency of the applied electric field. We show that the nonconductive component of the sample was eliminated in the normalized EIOC image. To the best our knowledge, this is the first time a two-dimensional image related to the electro-kinetic response of soft tissues is obtained with depth resolution. Since electro-kinetic properties can change during cancerogenesis, EIOC imaging can potentially be used for cancer detection.

OCIS codes: (110.4500) Optical coherence tomography; (170.2655) Functional monitoring and imaging; (170.6935) Tissue characterization; (170.7180) Ultrasound diagnostics.

http://dx.doi.org/10.1364/OL.38.002572

Many molecules, such as proteins and glycosaminoglycan on cell surfaces [1], or in the extracellular matrix of biological tissues, have net electric charges that can be described by a fixed charge density (FCD). Fixed charges cannot move around freely within the tissues when subjected to an electric field and therefore, do not contribute to conductivity. However, by interacting with the mobile ions in interstitial fluid, the fixed charges are responsible for various electro-kinetic phenomena (EKP) [2], which are the motion of particles and fluids under the influence of the electric field [3]. EKP depend on many tissue properties, such as the FCD, electrical conductivity, local pH variations, hydraulic permeability, ion diffusivity, and stiffness [4]. EKP have been observed using optical microscopy in colloids, blood, and cell cultures, such as changes in cellular shape [5], orientation [6], and migration (galvanotaxis) [7]. Frank and Grodzinsky measured the mechanical stress when the electric field was applied to the articular cartilage (a high FCD tissue) confined between two rigid plates [8,9]. Similarly, differential-phase reflectometry was used to monitor the electric field induced surface displacements of the cartilage tissue [10]. It was demonstrated that the magnitude of these surface displacements increased with amplitude and decreased with the frequency of the applied electric field.

EKP of various soft biological tissues have not been imaged with depth resolution until recently [11–13]. Ultrasound was used to image the electric-field induced mechanical changes (EIMC) in bulk tissues including deformation and strain one-dimensionally [12]. These EIMC in soft biological tissues were related to EKP [13].

Optical coherence tomography (OCT) allows for noninvasive, high-resolution, and depth-resolved imaging of internal tissue structure [14]. However standard structural OCT imaging cannot detect early pathological changes [15]. To investigate EKP in soft biological tissue, in this study we demonstrate that EKP can be imaged through the amplitude changes of OCT signals. To the best our knowledge, this is the first time a two-dimensional (2D) image related to the electro-kinetic response of soft tissues is obtained with depth resolution.

The experimental setup is shown in Fig. 1. The experimental protocol was similar to that of previous studies with ultrasound [11]. The tricuspid valves from the right ventricle of fresh porcine hearts were used as specimens. A rectangular tissue sample (~6 cm × 3 cm × 1.5 cm) was clamped into a Plexiglas frame to reduce random mechanical motion. Electrodes made of 24 AWG PVC hook-up 7 × 32 tinned copper wires (Copper Industries Belden Division, Richmond, IN) were placed 6 cm apart on the opposite sides of the surface of the sample (Fig. 1). To improve the electrical contact, each electrode was covered by the electrode gel Spectra 360 (Parker Laboratories, Inc. Fairfield, New Jersey). A synthetic function generator (Stanford Research, California, model DS335) was used to generate square-waves of 1–10 V amplitude and of 0.1–1.0 Hz frequency, which were applied to the electrodes. To minimize the effects of the temperature changes, the specimen was left at room temperature for 5 h before the experiment. The OCT system (Swept Source Laser Model no SL1325-P16, Thorlabs Inc. Newton, New Jersey) had a central wavelength of 1310 nm and the spectral bandwidth of 70 nm. The bandwidth was measured using the optical spectrum analyzer. The optical axial and transverse resolutions of the system were 10.8 and 25 μm (in air), respectively.

The electro-kinetic response of the tissue was initially investigated with M-mode OCT. 1024 consecutive M-mode A-scans with axial scan rate 16 kHz were acquired and then averaged to 1 A scan per second. Figure 2(a) shows the time course (480 s) of the relative amplitude

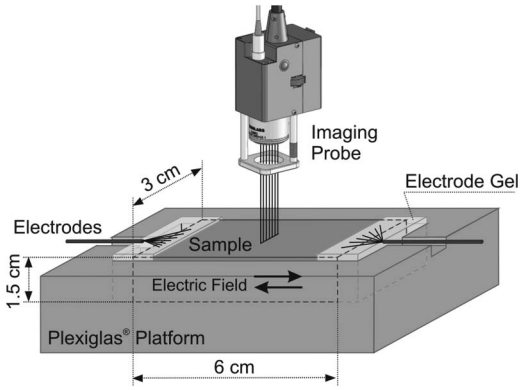

Fig. 1. Diagram of the experimental setup.

of the OCT signal normalized by the signal amplitude for one depth averaged over time. The AC voltage was applied only during the interval from 120 to 300 s, as indicated by the solid box. The amplitude of the OCT signal oscillates with the applied voltage. To study the linear response of the tissue to the applied field, Savitzky–Golay algorithm (sgolay function in Matlab, Mathworks, Natick, Massachusetts) was used to eliminate the slow trend (which is common in conventional optical swept sources [16]) in the signal [Fig. 2(a)]. The motivation for this detrending procedure was the elimination of the spurious frequencies in the spectrum of the signal from the trend. To quantify the electric-field induced optical changes (EIOC), a Fourier transform was first applied to the detrended signal during the interval of AC application. Then the magnitude of the Fourier spectrum at the frequency of the applied electric current [Fig. 2(c)] was used to represent the magnitude of EIOC. To investigate the dependence of EIOC on the applied voltage, 0.1 Hz AC square waves with various amplitudes from 1 to 10 V were applied to the sample. To investigate frequency dependence of EIOC, 10 V AC square waves were applied to the sample by varying frequencies from 0.1 to 1 Hz. To compare the changes in the OCT signal,

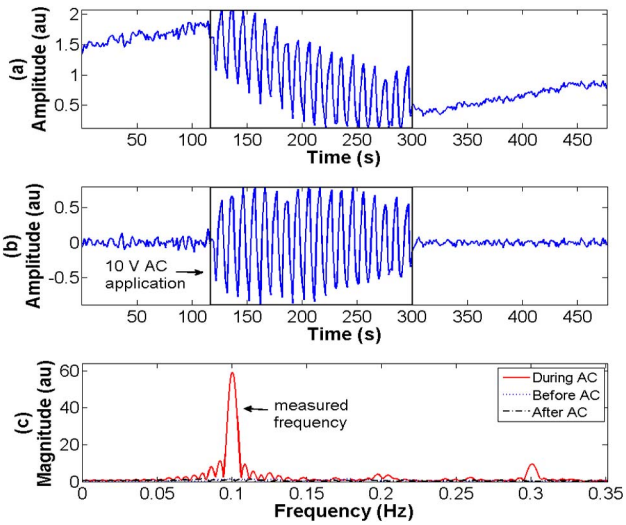

Fig. 2. (a) Time course of a typical OCT signal acquired on a sample before, during (inside the solid square), and after the AC voltage application, (b) same time course after detrending, and (c) Fourier spectrum of three portions of the signal.

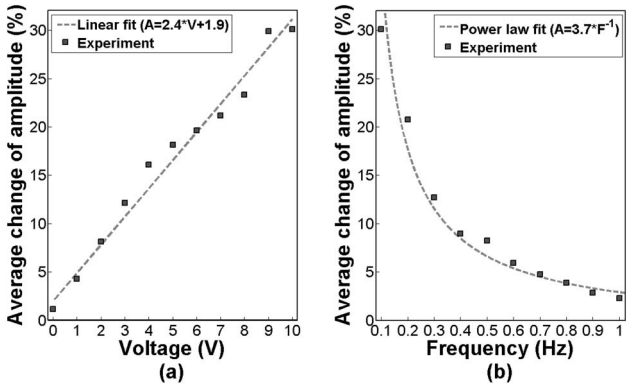

Fig. 3. Dependence of average EIOC amplitude on: (a) the amplitude and (b) the frequency of the applied voltage.

Fourier range of sample depths were averaged, and then converted to the percentage of amplitude change of OCT signals. The range of depths was selected from the surface of the sample to the depth below which the Fourier spectra peaks started to be dominated by noise. The EIOC amplitude dependence on the voltage is shown in Fig. 3(a), where a linear regression fit demonstrates that the EIOC magnitude increases linearly with the applied voltage. The EIOC amplitude dependence on the frequency is shown in Fig. 3(b). From Fig. 3(b) one can see that the EIOC magnitude is inversely proportional to the frequency of the applied electric field.

To investigate EIOC in 2D, a series of B mode OCT images (3×3 mm with 1024×512 pixels) were acquired with the rate of 0.064 s per image and 1 s between images. The 10 V, 0.1 Hz square-wave voltage was applied to the tissue during the time interval from 120 to 300 s. The signal processing technique was the same as in the one-dimensional case. Figure 4 illustrates the 2D image processing technique. For each (x, y) pixel of a B mode OCT image (1024 by 512 pixels), the temporal profile $A(t)$ [such as the plot in Fig. 2(a)] of the corresponding OCT signal during the application of external electric field ($t_{\text{start}} = 120$ s, $t_{\text{end}} = 300$ s) was extracted from the $A(x, y, t)$ matrix. Then a fast Fourier transform (FFT) was applied to the detrended signals to obtain the spectral magnitudes $S_f(x, y)$. Finally, $S_f(x, y)$, at the frequency $f_0 = 0.1$ Hz of the applied electric field, were mapped to the corresponding (x, y) pixels to construct an unnormalized EIOC image. The total processing time

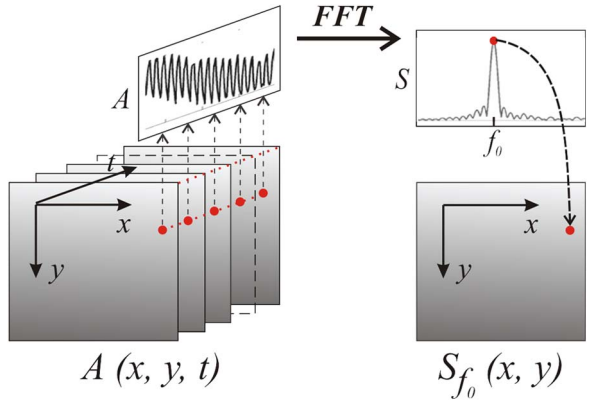

Fig. 4. Illustration of the EIOC image processing algorithm.

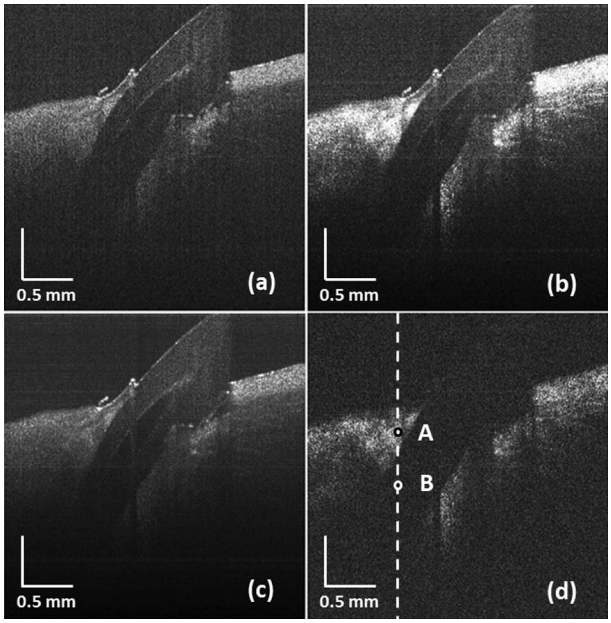

Fig. 5. (a) Original OCT image. (b) Unnormalized OCT-based EIOC image. (c) EIOC background image during electric field application. (d) OCT-based EIOC image normalized by the EIOC background image during electric field application.

for the 2D case was 12 min on an AMD Bulldozer 4.0 GHz 8 core system in Matlab.

To verify the ability of the technique to image the electro-kinetic response of tissues, a 1 mm diameter dielectric optical fiber was inserted into the middle of the sample at an arbitrary angle. Figures 5(a) and 5(b) display the structural and the unnormalized EIOC images, respectively. In both Figs. 5(a) and 5(b), the optical fiber cladding material surrounding the transparent core can be clearly distinguished.

Although no electro-kinetic response can occur in the optical fiber, the fiber is still visible in the EIOC image [Fig. 5(b)] because the background fluctuations of OCT signals gave rise to nonzero FFT values. To eliminate them from the EIOC image, a background image was computed using the FFT magnitude [Fig 2(b)] averaged over all the frequencies except the narrow bands around $f_0 = 0.1$ Hz and its corresponding harmonics. Then the EIOC image was divided by the background image, pixel-by-pixel. The result of this normalization is shown in Fig. 5(d). One can clearly see that the fiber and a small piece of surface tissue to the left of the fiber in Fig. 5(b) do not appear in Fig. 5(d), which is in agreement with the absence of electric current and EKP in them. It can also be concluded that the normalized EIOC image in Fig. 5(d) represents the information related to the local EKP of the tissue, rather than the one translated from other locations on the light pathway. Because if the EIOC were due to the changes in the path of the forward and backward light propagation, then any EIOC in top layer [for example, point A in Fig 5(d)] will result in the EIOC of the signal under that layer [point B in Fig 5(d)]. However, no EIOC of signal in the fiber glass region were detected, even though there are significant EIOC in the tissue above it.

Recently ultrasound imaging was used to investigate EIMC in biological tissues [11–13], including both the irreversible (strain) and reversible changes. In the current study, we report an observation of similar effects using OCT. Since the changes shown in Fig 2(a) are mostly reversible (opposite polarities of the applied voltage cause opposite OCT signal changes), it is unlikely that these changes were due to the strain, which is irreversible [13]. The result that the amplitude of the OCT signal increases with the amplitude [Fig. 3(a)] and decreases with the frequency [Fig. 3(b)] of the applied voltage is consistent with the results of the ultrasound imaging (after a frequency domain analysis of Figs. 5 (a) and 5(c) in [11]) as well as with those of the differential phase reflectometry [10] for the cartilage surface displacements. For the same level of applied electric field to tissue, we found that detected EIOC by OCT have a higher percentage of amplitude change than EIMC by ultrasound. The most likely reason for this is that the wavelengths of light used in OCT (about 1 μm) are much smaller than the wavelengths of ultrasonic waves (150 μm or greater), therefore OCT is more sensitive to the microscopic changes than the ultrasound. Since both ultrasound-detected EIMC and OCT-detected EIOC are reversible, they may have the same origin, probably due to the deformation of the extracellular matrix and cells, and due to the electrically induced fluid flow as discussed in [13].

This research was supported by NSERC discovery grants (Y. Xu and V. Toronov), CFI (V. X. D. Yang), MITACS (B. Vuong and C. Sun).

†The authors contributed equally to this work.

References

1. K. Thethi, P. Jurasz, A. J. MacDonald, A. D. Befus, S. F. Man, and M. Duszyk, J. Biochem. Biophys. Methods **34**, 137 (1997).
2. A. V. Delgado, F. González-Caballero, R. J. Hunter, L. K. Koopal, and J. Lyklema, J. Colloid Interface Sci. **309**, 194 (2007).
3. J. Lyklema, *Fundamentals of Interface and Colloid Science* (Academic, 2005).
4. W. Y. Gu, W. M. Lai, and V. C. Mow, in *Porous Media: Theory and Experiments* (Springer, 1999), Vol. **34**, pp. 143–157.
5. C. Katnik and R. Waugh, Biophys. J. **57**, 865 (1990).
6. S. Méthot, V. Moulin, D. Rancourt, M. Bourdages, D. Goulet, M. Plante, F. A. Auger, and L. Germain, Can. J. Chem. Eng. **79**, 668 (2001).
7. C. A. Erickson and R. Nuccitelli, J. Cell Biol. **98**, 296 (1984).
8. E. H. Frank and A. J. Grodzinsky, J. Biomech. **20**, 615 (1987).
9. E. H. Frank and A. J. Grodzinsky, J. Biomech. **20**, 629 (1987).
10. J. I. Youn, T. Akkin, and T. E. Milner, Physiol. Meas. **25**, 85 (2004).
11. O. Doganay and Y. Xu, in *IEEE International Ultrasonics Symposium* (IEEE, 2009), pp. 2103–2106.
12. O. Doganay and Y. Xu, J. Acoust. Soc. Am. **128**, EL261 (2010).
13. O. Doganay and Y. Xu, IEEE Trans. Ultrason. Ferroelectr. Freq. Contr. **59**, 552 (2012).
14. J. G. Fujimoto, C. Pitris, S. A. Boppart, and M. E. Brezinski, Neoplasia **2**, 9 (2000).
15. A. F. Fercher, W. Drexler, C. K. Hitzenberger, and T. Lasser, Rep. Prog. Phys. **66**, 239 (2003).
16. D. C. Adler, R. Huber, and J. G. Fujimoto, Opt. Lett. **32**, 626 (2007).